Novelty Journals

ISSN 2394-9651

International Journal of Novel Research in Physics Chemistry & Mathematics
Vol. 11, Issue 3, pp: (1-9), Month: September - December 2024, Available at: www.noveltyjournals.com

First Principle Computation of Monolayer-$NbSe_2$: Structural, Electronic and Optical Properties

Aqeel Mohsin Ali

Polymer Research Center – University of Basrah – Basrah – Iraq

DOI: https://doi.org/10.5281/zenodo.13839422

Published Date: 25-September-2024

Abstract: **An investigation of the structural, electrical, and optical properties of a monolayer of two-dimensional $NbSe_2$ is carried out with the assistance of the density functional theory. For the purpose of ensuring the structural and thermal stability of the monolayer, it is essential to ascertain the binding energy in addition to the phonon spectra. Through the use of first-principles simulations, we have investigated the electrical and optical properties of monolayers of $NbSe_2$ material. $NbSe_2$ monolayers have been shown to possess inherent properties that make them desirable for usage as two-dimensional materials in nanoelectronics applications. This discovery was made possible by the nature of the monolayers themselves. In addition, the optical properties of the $NbSe_2$ monolayers that were investigated for their two-dimensional applications are computed and described. These optical properties include the optical absorption coefficient, optical conductivity, reflectivity, and energy loss function.**

Keywords: **$NbSe_2$ monolayer, DFT, Band structure, Optical properties, metallic $NbSe_2$, Transition metal dichalcogenides.**

I. INTRODUCTION

The materials that are two-dimensional (2D) have arisen as a unique category of nanomaterials with different physical and chemical features. This come about as a result of the discovery of graphene in 2004 by A. Geim and K. Novoselov [1]. Honeycomb-like structure that is defined by sp^2 hybridization is shown by graphene. In addition to this, it has outstanding stability and possesses distinctive electrical properties, such as very high strength, tremendous flexibility, and enhanced carrier mobility[2-4]. Although graphene is a fantastic material, the fact that it behaves like a semiconductor with zero band gap limits the applications that it may potentially have in modern electrical systems. Because of the outstanding successes of graphene, researchers have begun to focus more of their attention on other two-dimensional materials, such as borophene, transition metal dichalcogenides (TMDs), stanene, and other materials [5-9]. There is a category of two-dimensional materials known as transition metal dichalcogenides, or TMDs for short. These materials have emerged as formidable competitors in the sector. There is a general formula for them that is MX2, where M stands for a metal and X2 stands for atoms of dichalcogenide. These materials have a band gap that is direct and may vary anywhere from 1 to 2.5 eV [10]. Due to the varied characteristics of TMDs, several researchers have documented their usage in various applications such as photocatalysis, optoelectronics, photovoltaics, sensors, and solar cells [10-12]. As far as we know, there is currently no existing literature on the thermal characteristics of a stretched monolayer of $NbSe_2$.

Hence, the investigation of the electrical and optical characteristics is conducted. In addition, the phonon dispersion curve characteristics are examined.

Novelty Journals

ISSN 2394-9651

International Journal of Novel Research in Physics Chemistry & Mathematics
Vol. 11, Issue 3, pp: (1-9), Month: September - December 2024, Available at: www.noveltyjournals.com

II. COMPUTATIONAL DETAILS

The CASTEP algorithm utilizes Density Functional Theory (DFT) to explore the structural, electrical, and thermal characteristics of the $NbSe_2$ Monolayer [13]. To explore the correlation and exchange interaction, we used norm conserving, pseudopotential, and GGA-PBE functional [14]. Upon using the CG methodology to optimize the structure, we determined that the force tolerance amounted to 0.0001 eV/Å. We have used Plane Wave basis sets with a confinement energy of 20 meV and a cut-off energy of 350 Ry mesh. A Monkhorst-Pack k-point grid of 9×9×1 was utilized to integrate the Brillouin zone in two dimensions. The phonon spectra and thermal properties are calculated using the small displacement method. The electronic band structure, partial density of states, and optical characteristics are examined using the same theoretical framework.

III. RESULT AND DISCUSSION

In order to optimize the unit cell, we used three atoms per unit cell (one Nb atom and two Se atoms), as seen in Figure 1, and we estimated the structural parameters using the information provided in table I. The lattice constant and bond length for $NbSe_2$ ML have been predicted to be 3.46 Å and 2.60 Å, each in order. These values are considered to be through with the existing theoretical [15] and experimental evidence [16]. The distance between the two Se atoms is measuring to the monolayer thickness, which has the value of 3.33 Å. Furthermore, in order to determine whether or not the $NbSe_2$ monolayer is stable, we computed the binding energy, which is defined as follows:

$$BE = 0.333 \times (E_t - E_{Nb} - 2E_{Se})$$

The variable E_t illustrates the overall energy of the framework. E_{Nb} refers to the energy of the transition atom Nb, while E_{Se} represents the energy of the chalcogen atom. Greater binding energy corresponds to increased stability. The predicted binding energy for a monolayer of $NbSe_2$ is 4.86 eV per atom.

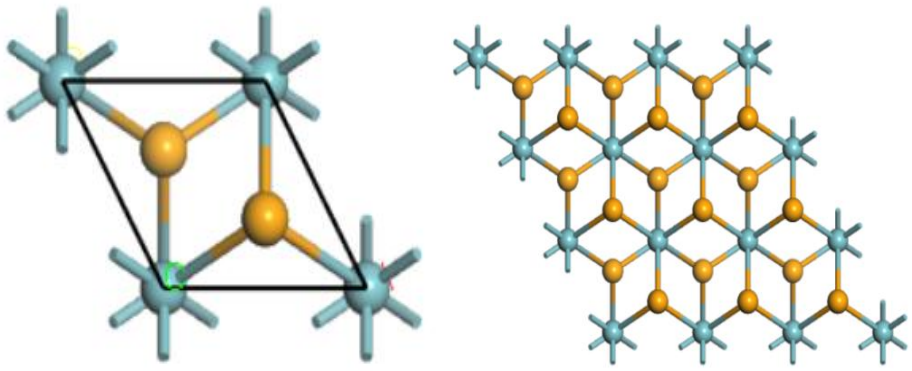

Fig. 1: $NbSe_2$ monolayer (a) Unit cell (b) 3×3 supercell.

Table I: Lattice constant a_0, bond length BL, binding energy BE and Se-Se distance of $NbSe_2$ ML.

Monolayer	a_0 (Å)	BL (Å)	BE (eV)	Se-Se (Å)
$NbSe_2$	3.46 3.45 [15] 3.57 [16]	2.60 2.60 [15] 2.65 [16]	4.86 4.85 [15]	3.33

Figure 2 displays the phonon dispersion curve for $NbSe_2$ ML. In the first Brillouin zone, all of the phonon frequencies for the $NbSe_2$ monolayer are positive, suggesting that this structure is dynamically stable. Figure 2 shows that there are three acoustic modes and six optical modes created by the three atoms in the unit cell. There are three distinct acoustic modes: the compressional wave-corresponding longitudinal (LA) mode, the shear wave-corresponding transverse (TA) mode, and the out-of-plane atomic displacement-corresponding acoustic (ZA) mode.

Novelty Journals

ISSN 2394-9651

International Journal of Novel Research in Physics Chemistry & Mathematics
Vol. 11, Issue 3, pp: (1-9), Month: September - December 2024, Available at: www.noveltyjournals.com

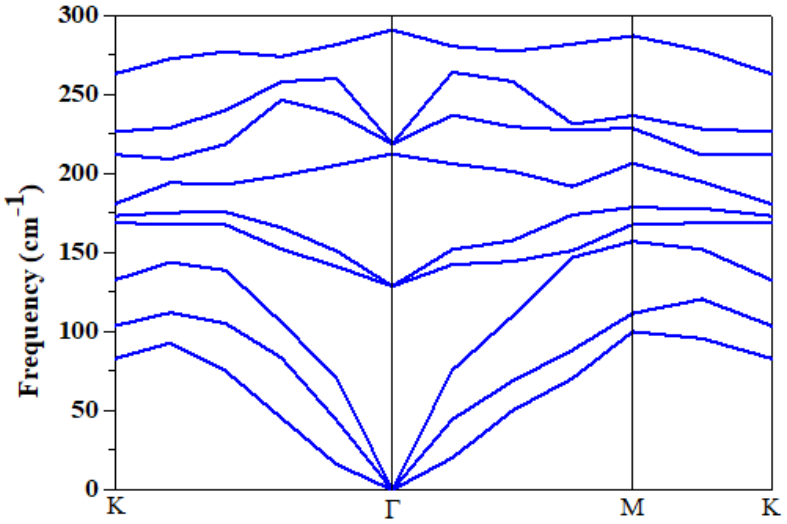

Fig. 2: phonon dispersion curve for $NbSe_2$ ML.

Contrarily, Single-layer $NbSe_2$ exhibits a much more straightforward anticipated arrangement of electrons (Figure 3). It consists of just one band originating from Nb that intersects Fermi energy level (E_F) away from the Γ point. The computed dispersion is a reflection of a variety of states, with the high-symmetry directions Γ-M and Γ-K being the sources of the dominating intensity. At the intersection of E_F, two dispersive characteristics may be seen. Additionally, it has a bandgap ranging from -0.54 to -0.87 eV, with valence bands located below it. The anticipated characteristics are evident in Ugeda et al. experimental results the bandgap ranging from -0.4 to -0.8 eV. The dispersion reveals that states just below the Fermi energy (E_F) are situated at a distance from the Γ point, and many valence bands are present below -0.87 eV.

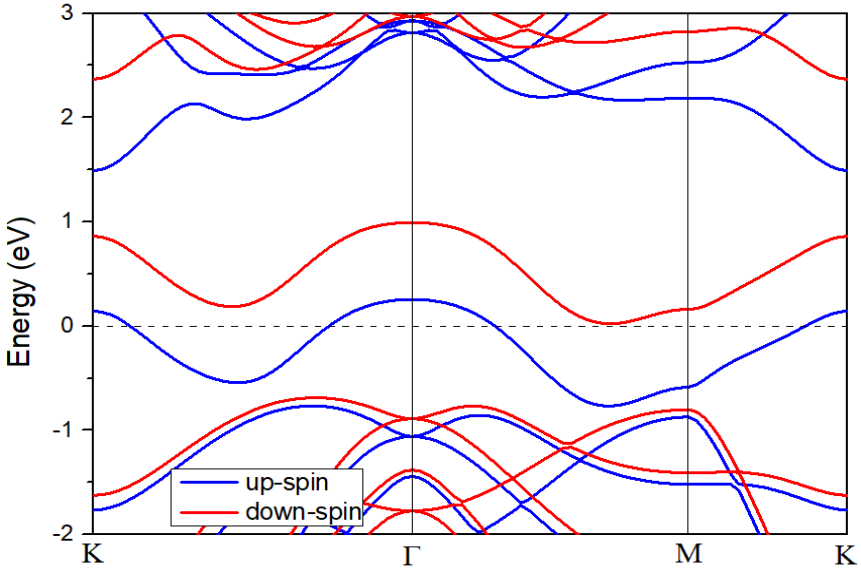

Fig. 3: Spin dependent electron band structure of $NbSe_2$ ML.

In order to examine the spin-dependent electrical characteristics of $NbSe_2$ monolayer, we conducted calculations on the spin-dependent band structure and total density of states (TDOS), as seen in Figure 4 (a). It has been discovered that the spin of $NbSe_2$ is metallic, with a greater number of possible states for the down spin at the fermi level. The metallic kernel

of $NbSe_2$ monolayer is attributed to the overlapping of the selenium (Se) *p*-orbital and the niobium (Nb) dz^2 orbital as shown in figure 4 (b), which intersect the Fermi level. The PDOSs that were calculated for Nb and Se demonstrate a dominant role in relation to E_F. Nevertheless, these states are somewhat more extensive in energy (ranging from -6 eV to 1 eV), and they are visible in the energy range that is essentially comparable. These states disclose the covalent character of the materials that are being investigated as a result of the significant hybridization that occurs between the cation and anion atoms. The electronic structures of $NbSe_2$ single-layer were established by experimental measurements of low-temperature transport and ARPES, which contrasted with the experimental report of Ugeda et al. [17]. In this study, it was shown that the electronic band structures of $NbSe_2$ single-layer are solely derived from Nb around the E_F. The total density of states (TDOS) for Nb states has a maximum value of around 0.21 eV downward for E_F. With the exception of a few peaks seen around E_F up to 0.2 eV, DOS displays a gradually decreasing function. The electronic states subsequent to this energy range are attributed to niobium with a little contribution from selenium. These results support the previous experimental investigation, which found a reduced quasi-gap of about 4 meV in the observed spectra at zero voltage. This phenomenon is attributed to the distortion caused by the CDW.

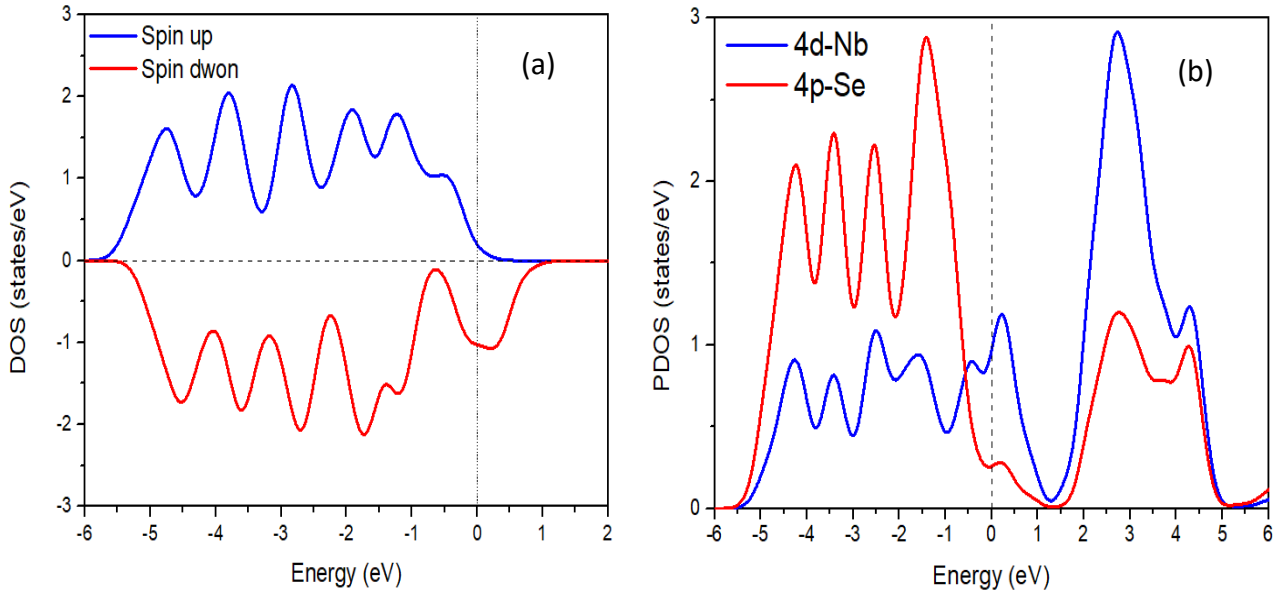

Fig. 4: Spin dependent electron density of states of $NbSe_2$ML. (a) Total DOS and (b) partial

The investigation of the optical characteristics may be defined by analyzing the interaction between light-radiation and a solid with respect to the primary parameter, namely the dielectric function. The critical factor is associated with the electronic structures of a material and their examination in optical spectroscopic data. Indeed, the dielectric function is partitioned into two significant components, namely the real and imaginary. The equation $\varepsilon(\omega) = \varepsilon 1(\omega) + i\varepsilon 2(\omega)$ is used to describe the electronic-radiation spectrum response of a material. By analyzing the spectrum characteristics of the real and imaginary components of $\varepsilon 2(\omega)$, it is possible to assess the computational properties of other optical spectra, such as the optical absorption coefficient, reflectivity, refractive index, energy loss function, and others.

Determine the dielectric function for the electric field vector that is polarized parallel to the crystallographic c-axis. The spectra of $\varepsilon 1(\omega)$ in Figure 5 show a shoulder at 0.69 eV, which thereafter descends to a first critical point at 0.00 eV. These results once again demonstrate the inherent zero band gap characteristic of metallic $NbSe_2$ monolayer, as previously mentioned in band structure and PDOS shown in Figures 3-4. The first critical point of $\varepsilon 2(\omega)$ is 0.00 eV, in close proximity to the computed metallic band gap and often referred to as the fundamental absorption edge. This observation validates the occurrence of the intraband transitions from the intersection line Σ (in the direction K-Γ) toward Γ point. The spectra of $\varepsilon 2(\omega)$ exhibit a conspicuous and substantial peak at 3.15 eV. The $\varepsilon 1(\omega)$ spectrum has a solitary minor peak at 8.94 eV and a shoulder at 12.5 eV and so on. In contrast, the $\varepsilon 2(\omega)$ spectrum displays a single minor peak at

9.42 eV. With a peak at around 8.94 eV, the transition from Nb 3d to Se 5s orbitals might be the key. The major source of the peak at 12.5 eV is the transition between the 3d and 5s orbitals of niobium and selenium. The peaks at around 9.42 eV are attributed to the Se 4p and Nb 5s states.

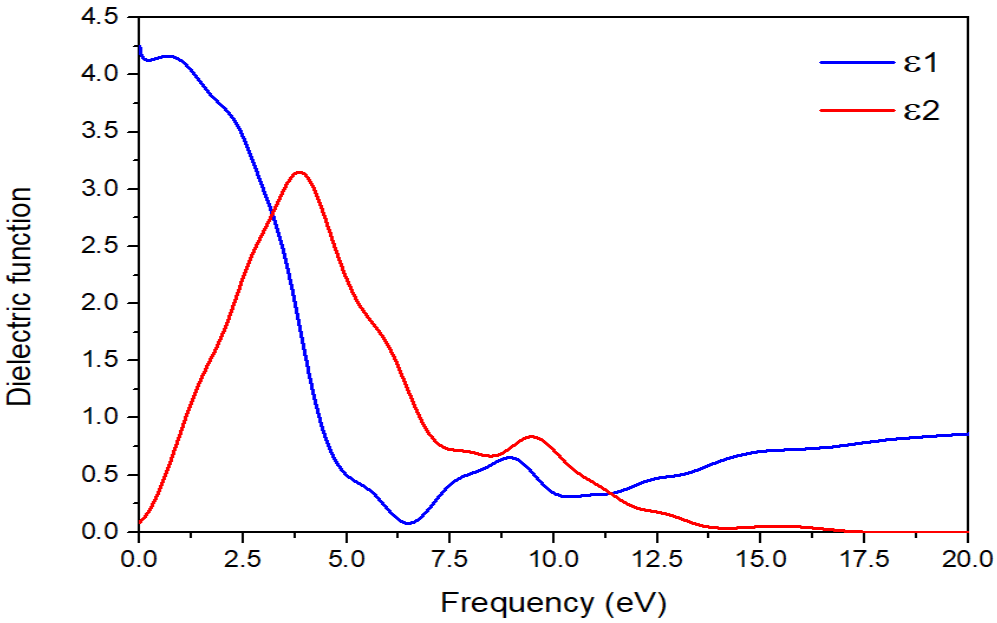

Fig. 5: Dielectric function parts of $NbSe_2$ ML.

Analyzing the absorption coefficient spectrum provides a more comprehensive insight into the electrical structural characteristics of the two-dimensional materials being investigated. Pure $NbSe_2$ monolayer optical absorption spectra calculated at electromagnetic radiation energy up to 20 eV are shown in Figure 6, as is evident. The optical absorption coefficient spectrum of a single layer of pure $NbSe_2$ indicates a peripheral optical absorption at low photon energy. This is due to the fact that the spectral feature begins in the infrared region, and the absorption edge is about around 1.0 eV. This is something that is easily observable. Figure 6. When it comes to this particular material, the high absorption happens at the intermediate photon energy linked with the energy values that range from 2.5 to 6.5 eV. The second regime is characterized by the presence of considerable optical absorption for photon energy levels that raised up within the range of 9.0 to 12.5 electron volts. Within the third part, which spans from 14 to 17.5 eV, there is a significant absorption that may be seen.

Figure 7 illustrates the both real and imaginary components of the relationship between optical conductivity and frequency. The analysis of this figure reveals that the real component exhibits a positive correlation with frequency, but the imaginary component reaches an energy level (equivalent to the optical bandgap, $h\nu$ = 2.6 eV = E_g^{opt}) and thereafter declines. A noteworthy outcome of negative imaginary conductivity is the reversal of the direction of current density prior to reaching its equilibrium value of zero. The rise in the extinction coefficient is the source of the negative value of the imaginary portion of optical conductivity. This value indicates that there is a decrease in the conductivity of the $NbSe_2$ monolayer, and similar to that, there is a decrease in the propagation of electromagnetic waves within this area. The carrier localization in semiconductor alloys may be attributed to the potential fluctuations caused by composition inhomogeneity, which accounts for the negative imaginary portion of optical conductivity. The phenomenon of alloy dispersion, which exists even in an exemplary alloy, serves as an additional means to augment this region of localization.

Novelty Journals

ISSN 2394-9651

International Journal of Novel Research in Physics Chemistry & Mathematics
Vol. 11, Issue 3, pp: (1-9), Month: September - December 2024, Available at: www.noveltyjournals.com

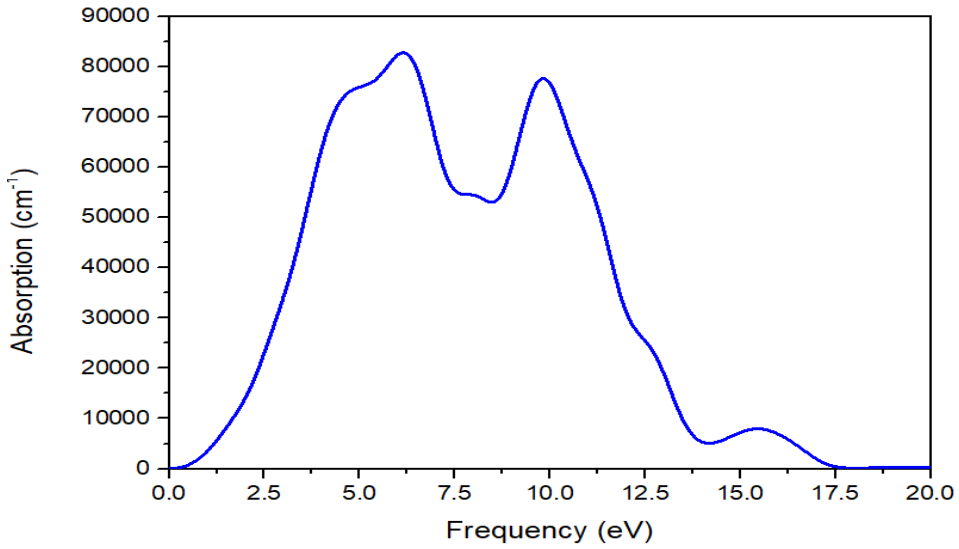

Fig. 6: Absorption curve of $NbSe_2$ ML.

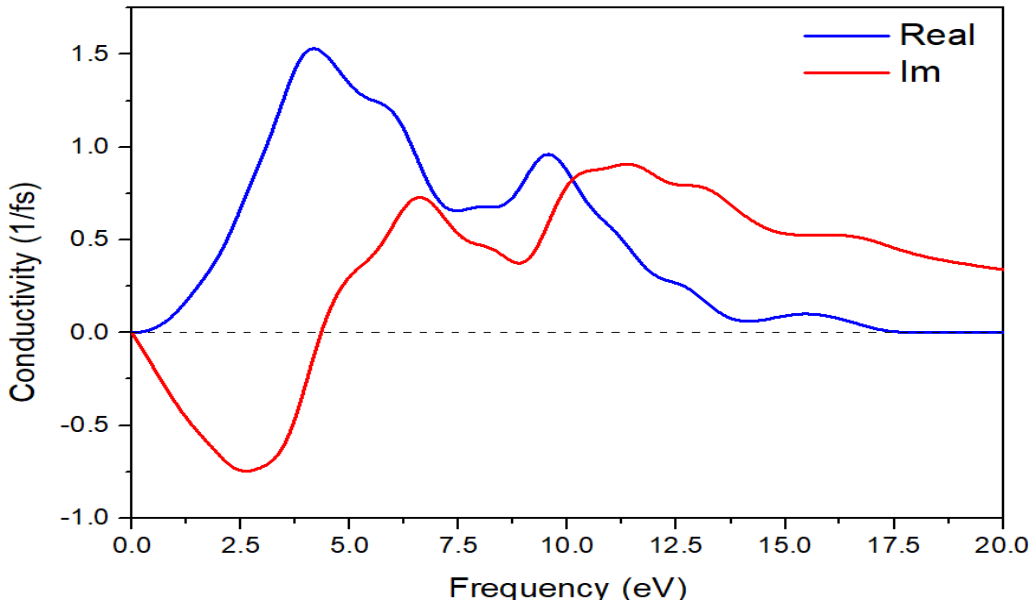

Fig. 7: Optical conductivity of $NbSe_2$ ML.

Reflectivity is a fundamental topic related to the optical properties of solids. In this study, we analyze the linear optical behavior by examining the transitions in normal incident reflectivity between the valence bands and the downward conduction bands. In Figure 8, the optical spectrum constituents of reflectivity are shown within the photon energy domain of 0–20 eV. As demonstrated in Figure 8, the reflectance of the $NbSe_2$ sheet is remarkably 0.12 at zero energy. Moreover, a notable reflectivity was observed throughout the range of IR and visible-UV light (0 → 7 eV). In the range of UV-electromagnetic radiation (8 → 13 eV), the presence of the medium of peaks reflectivity is established. Furthermore, the reduced reflectivity is realized throughout the range of 15 → 20 eV for the monolayer system. The significant reflection observed for energy levels below 1.5 eV indicates the characteristic of strong conductivity within the lower energy bandwidth. Drude type analysis indicates that the $NbSe_2$ monolayer exhibits a metallic character outwardly the participation of excitons.

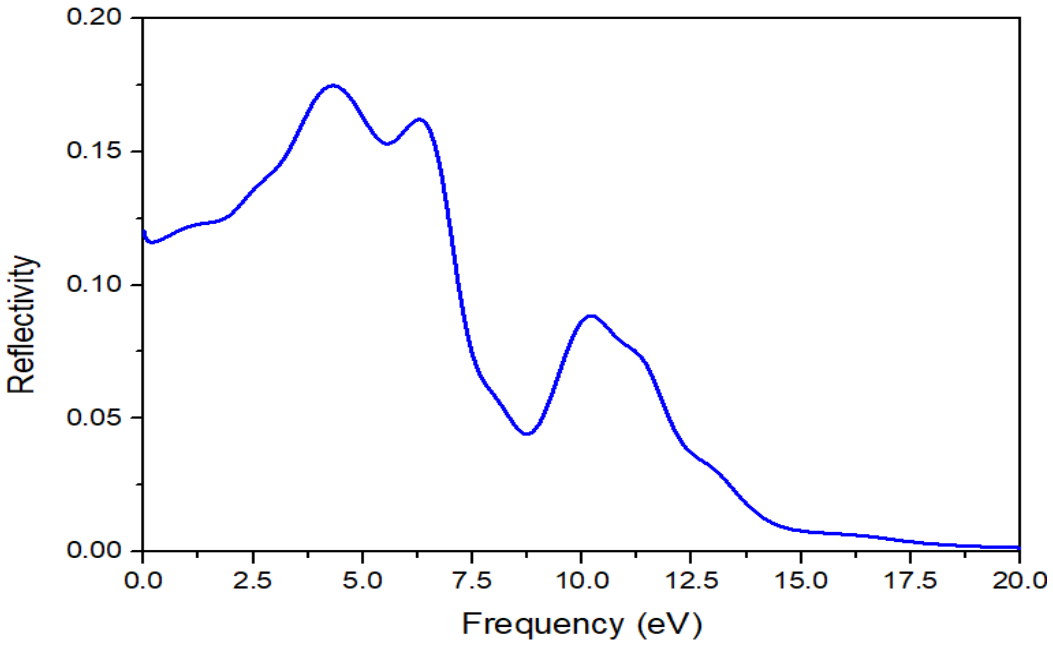

Fig. 8: Reflectivity curve of $NbSe_2$ ML.

Valuable for examining the energy dissipation of a rapid electron as it traverses the transmission medium. Characteristic peaks in the spectra of loos function arise from the plasma resonance occurring at the plasma frequency ω_P [18]. Figure 9 illustrates that the energy loss curve starts at 0 eV and increases linearly up to 2 eV for the $NbSe_2$ monolayer. The energy losses function is determined for the system being studied with an energy domain spanning from 0 to 20 eV. We see prominent plasmon peaks of loos function at around 14.5 on the $NbSe_2$ sheet. The squeaky spectral crest locations of loos function are shown in Figure 7 and are settled between 12 and 15.5 eV. Hence, the dissipation of energy occurs roughly within the photon energy range of 17.5–20 eV. Recent analysis of electron energy loss spectra for $NbSe_2$ monolayer indicates that plasmons are excited at an energy of around 14.7 eV. Through an analysis of the fluctuations in loos function of the $NbSe_2$ monolayer, we observed a shift of the peak of plasmons at 14.9 eV [19].

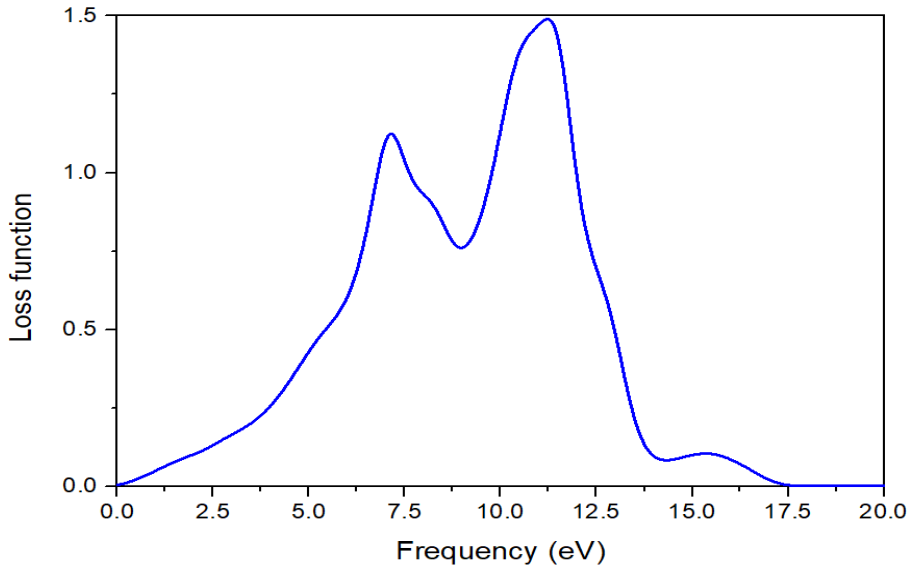

Fig.9: Loos function curve of $NbSe_2$ ML.

IV. CONCLUSIONS

The electronic and optical properties of the freestanding $NbSe_2$ monolayer were examined using the LAPW technique of Density Functional Theory (DFT). The computed partial density of states (DOS) plots have shown that the Nb 4d and Se 4p orbitals are mostly accountable for the division of the states concerning the Fermi energy (E_F). Through the analysis of optical spectrum functions, it has been shown that the absorption of the pure $NbSe_2$ monolayer is generally modest when exposed to low photon energy. The optical conductivity is shown to align with a straightforward Rude model, characterized by the presence of Drude peaks across the mid-infrared range. It is suggested that the energy loss function has significant plasmon peaks L (ω), which appear at about 14.9 eV.

REFERENCES

[1] K. S Novoselov, A. K Geim, S. V Morozov, D. jiang, Y. Zhang, S.V. Dubonos, I.V. Grigorieva and A.A Firsov. "Electric field effect in atomically thin carbon films", Science, Vol. 306, pp. 666-669, 2004.

[2] A. H. Castro Neto, F. Guinea, N. M. R Peres, K. S. Novoselov and A. K Geim, "The electronic properties of graphene", Review Modern Physics, Vol. 81, pp. 109-162, 2009.

[3] K. S. Novoselov, A. K. Geim, S. V. Morozov, D. Jiang, M. I. Katsnelson, I. V. Grigorieva, S. V. Dubonos and A. A Firsov, "Two dimensional gas of massless Dirac fermions in graphene", Nature, Vol. 438, pp. 197-200, 2005.

[4] A. M. Ali, "A Electron transport study on ultrathin armchair graphene nanoribbone", Journal of Kufa-Physics, Vol. 11, No. 2, pp: 62-72, 2019.

[5] T. Vishal, K. Narender, B. K. Rao, M. L. Verma, H. D. Sahu; V. Swati and C. Anil Kumar, "Density functional study on hybrid graphene/h-BN 2D sheets", Physica E: Low-dimensional Systems and Nanostructures, Vol. 133, pp. 114-812, 2021.

[6] N. Kumar, N. Saleh and N. Tit, "Magnetization in CNT induced by nitrogen doping and enhanced by transversal electric field application", Journal of Material Science, Vol. 57, pp. 9277–9298, 2022.

[7] B. Chettri, P. K. Patra and M. Lalmuanchhana, "Induced magnetic states upon electron–hole injection at B and N sites of hexagonal boron nitride bilayer: A density functional theory study", International Journal of Quantum Chem, Vol. 2201, pp. 121:26680, 2021.

[8] A. M. Ali, "Ab initio Study of the Electronic and Optical Properties of Stable Boron Sheet", Iraqi Journal of Science, Vol. 62, No. 12, pp: 4687-4693, 2021.

[9] A. M. Ali, "Investigation of Aluminum Arsenide Honeycomb Monolayer via Density Functional Theory", Iraqi Journal of Science, Vol. 64, No. 1, pp: 197-204, 2023.

[10] V. Sorkin, H. Pan, H. Shi, S. Y. Quek and Y. W. Zhang, "Nanoscale Transition Metal Dichalcogenides: Structures, Properties, and Applications", Critical Reviews in solid state and materials sciences, Vol. 39, pp. 319-367, 2014.

[11] K. Zhang, Y. C. Lin and J. A. Robinson, "Synthesis, properties and stacking of Two-dimensional Transition metal dichalcogenides", Semiconductor semimetals, Vol. 95, pp. 189-219, 2016.

[12] X. Chen and A. R. McDonald, "Functionalization of two-dimensional transition metal dichalcogenides", Advanced material, Vol. 28, pp. 5738-5746, 2016.

[13] S. J. Clark, M. D. Segall, C. J. Pickard, P. J. Hasnip, M. I. J. Probert, K. Refson, and M. C. Payne, "First principles methods using CASTEP," *Zeitschrift für kristallographie-crystalline materials*, Vol. 220, No. 5-6, pp. 567-570, 2005.

[14] J. P. Perdew, A. Ruzsinszky, G. I. Csonka, O. A. Vydrov, G. E. Scuseria, L.A. Constantin, X. Zhou and K. Burke, "Restoring the density-gradient expansion for exchange in solids and surfaces", Physical review letters, Vol. 100, 136406, 2008.

[15] K. Ashutosh, A. Devi, A. Kumar, A. Singh and R.. Adhikari, "Structural, electronic and thermal properties of $NbSe_2$ monolayer: First principle study", Vol. 12, January 020104, 2024.

[16] J. A. Wilson and A. Yoe, "The transition metal dichalcogenides discussion and interpretation of the observed optical, electrical, and structural properties", Advance Physics, Vol. 18, pp. 193-335, 1969.

[17] M. M. Ugeda, A. J. Bradley, Y. Zhang, S. Onishi, Y. Chen, W. Ruan, C. Ojeda-Aristizabal, H. Ryu, M. T. Edmonds, H. Tsai, A. Riss, S. Mo, D. Lee, A. Zettl, Z. Hussain, Z. Shen and M. F. Crommie, "Characterization of collective ground states in single-layer $NbSe_2$", Nature Physics, Vol. 2, November 2015.

[18] H. Li, S. Liu, L. Chen, J. Wu, P. Zhang, H. Tang, C. Li, X. Liu, Z. Wang and J. Meng, "Atomic structures and electronic properties of Ta-doped 2H-$NbSe_2$", RSC Advances, Vol. 4, 57541, 2014.

[19] J. Guo, Y. Shi, C. Zhu, L. Wang, N. Wang and T. Ma, "Cost-effective and morphology-controllable niobium diselenides for highly efficient counter electrodes of dye-sensitized solar cells", Journal of Material Chemistry A, Vol. 1, pp. 11874-11879, 2013.